Magazine of Civil Engineering

ISSN 2712-8172

journal homepage: http://engstroy.spbstu.ru/

DOI: 10.34910/MCE.110.9

The behaviour of thin-walled beam with restrained torsion

V.V. Galishnikova [a], ***T.H. Gebre*** [b]*

[a] *National Research Moscow State Civil Engineering University, Moscow, Russia*

[b] *Peoples' Friendship University of Russia, Moscow, Russia*

**E-mail: tesfaldethg@gmail.com*

Keywords: thin-walled structures, restrained torsion, section properties, angle of twist, open section, closed sections, non-uniform warping, torsional stress

Abstract. In this paper, the behaviour of thin-walled sections of a bar with restrained torsion is studied. Neglecting these warping behaviours may generate significant errors, particularly for open profile torsion or shear bending of short beams. The governing equation for non-uniform torsion is used to study the behaviour of the beam with restrained torsion. The variation of the primary torsional moment, secondary torsional moments and warping moments for different value of characteristic number for torsion are presented graphically. Finally, the behaviour and comparison of all torsional moment components with three different thin-walled sections are illustrated by presenting and discussing their results. The section properties, displacements, rotations, stresses and their distribution within the span are compared based on the required value of characteristic number for torsion. It is found that for all thin-walled sections, the characteristic number for torsion is the key criteria for the study of the behaviour of thin-walled sections of a bar with restrained torsion.

1. Introduction

The behaviour of a bar with restrained torsion differs significantly from stretching and bending moreover their mathematical formulations varies. In analyses of thin-walled structures subjected to torsion, the effect of warping must be considered as the axial stresses mainly occur at the points of action of concentrated torsion moments (except for free ends) and at sections with warping restraints. The most profitable and effective way to construction of prefabricated structures is to use the system of light steel thin-walled structures, and also thermal insulation, facing and vapor sealing [1]. Normally, thin-walled sections do not behave according to the law of the plane sections employed by Euler-Bernoulli-Navier however the general theory of thin-walled section developed by Vlasov [2]. If warping is not restrained, the applied twisting moment is entirely carried by uniform torsion as a result the shear contribution to the deformation energy can be considered small enough [3–4]. Torsion leads not only to cross-section rotation about the centre of twist but at the same time the points of the section undergo different displacements along the longitudinal axis [5]. For warping restrained, the member develops additional shearing stresses, as well as normal stresses as warping stresses are not to be ignored [6–7]. The resulting stresses are primarily shear stresses (uniform torsion) or a combination of shear and longitudinal stresses (non-uniform torsion). The distribution of these stresses through the thin-wall section depends to a large extent on the cross sectional geometry and specifically whether it is open or closed sections [8]. In order to include warping shear stresses in the global equilibrium of the bar, that is to account for the secondary torsional moment deformation effect, an additional kinematical component (along with the angle of twist) is generally required, increasing the difficulty of the problem at hand [9].

Remarkable growth has been made since the 1945s in classical theories of torsion of thin-walled beams members with the consideration of warping, but it was limited to symmetric cross sections due to its complexity. There are many studies on non-uniform torsion with or without consideration of warping effects

Galishnikova, V.V., Gebre, T.H. The behaviour of thin-walled beam with restrained torsion. Magazine of Civil Engineering. 2022. 110(2). Article No. 11009. DOI: 10.34910/MCE.110.9

as theories and also as analysis using commercial FEM codes [8–16]. Similarly, researchers worldwide have extensively used fibre-reinforced polymer (FRP) strengthening materials to enhance the combined load strengths of reinforced concrete (RC) beams [18–23]. It has various well-known advantages such as high strength to weight ratio, high corrosive resistance, and easy-to-apply character [24]. The effect of span length of cantilever RC beams under pure torsion had been studied using a non-linear finite element analysis [25]. The element stiffness matrix and load vectors are derived using the primary and secondary warping functions [17–18]. Warping effects occur mainly at the points of action of the concentrated torsional moments (except for free beam ends) and at sections with free-warping restrictions [19–20]. The warping effect was included through an additional degree of freedom at each nodal point in the form of the first derivative of the angle of twist of the cross-section of the beam [10, 21]. Meanwhile, the torsional analysis of thin walled sections including shear has been studied in Ref. [15, 22–26]. The analysis of uniform torsion shows that the warping of bars depends on the shape of their section. A new torsion element of thin-walled beams including shear deformation which accounts for the warping deformation and shear deformation due to restrained torsion is developed [27–28]. Prismatic bars of solid and hollow sections or thin-walled section with a single interior vertex (for example an angle, a tee or a cross) do not warp but all other sections will experience warping of the cross section, depending on the geometry of the cross section [38]. Neglecting these warping stresses may generate significant errors specially for open profile torsion or shear-bending of short beams, and the situation may be even more critical for composite beams [6–7]. Warping-based stresses and deformations in closed sections, however, are assumed to be insignificant and have been therefore neglected [39]. Reasonably strong warping is expected to have effect in open than closed cross-sections and its significance is anticipated to be restricted to open cross-sections. Restraining the warping deformation causes the twist rate to be zero at the point of restraint and this causes a local effective torsional stiffening that affects the global torsional response of the beam [40]. The difference between the displacements and stresses due to uniform and non-uniform torsion is most pronounced for thin-walled sections. Warping of a thin-walled structures due to torsion stands for all the longitudinal displacements caused by the torsional rotation of the member cross-section around its shear centre. Thin-walled beam, because of its specific properties, has a unique internal force factor – bi-moment, which in certain cases can cause large normal stresses in cross-section [41].

In this paper, the behaviour of thin-walled sections of a bar with restrained torsion using the governing equation for non-uniform torsion is considered. This study is extensively applied to bars of closed and open sections of thin-walled steel cross section subjected to concentrated torsional loading and to the most general torsional boundary conditions. The variation of primary torsional moment $\left(\mathrm{M_{TP}}\right)$, secondary torsional moments $\left(\mathrm{M_{TS}}\right)$ and warping moments $\left(\mathrm{M_{\omega}}\right)$ for different value of characteristic number for torsion $\left(\theta\right)$ are presented graphically. Finally, the behavior and comparison of all torsional moment components with three different thin-walled sections are illustrated by presenting and discussion their results.

2. Methods

2.1. Defining Governing Equations

The governing equation for non-uniform torsion is used to study the behaviour of a bar with restrained torsion and it is derived for bars with thin-walled sections with local coordinate systems $\mathrm{y_1}, \mathrm{y_2}, \mathrm{y_3}$ as shown in Fig. 1 [31].

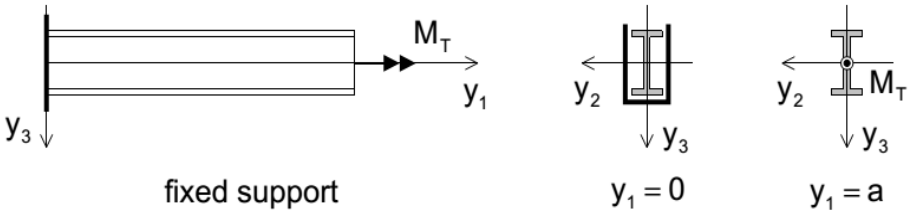

Figure 1. Torsion of prismatic bar.

When the bar is subjected to the arbitrarily distributed twisting moment $\mathrm{M_T}$ and its angle of twist is defined by the following governing equation (2.1) with boundary value problem [13, 18, 34, 42].

$$\frac{dM_T}{dy_1} + m_T = 0,$$
$$EC_\omega \frac{d^4\beta_1}{dy_1^4} - GJ\frac{d^2\beta_1}{dy_1^2} = m_T, \tag{2.1}$$

where β_1 is angle of twist, E, G are elastic constant, C_ω is warping constant, J is torsion constant, m_T is twisting load per unit length of bar.

If a bar undergoes non-uniform torsion, the total applied twisting moment $\mathrm{M_T}$ is resisted by an internal twisting moment that consists of two components as given in equation (2.2). The primary internal moment is the twisting moment $\mathrm{M_{TP}}$ due to uniform torsion (St Venant torsion). The secondary internal moment is the twisting moment $\mathrm{M_{TS}}$ is due to warping restraint and the twisting moments are expressed in terms of the angle of rotation β_1 and the properties of the shape of the section. The applied torque is resisted by a combination of the uniform and warping torques and it is given with its differential equation of non-uniform torsion.

$$\mathrm{M_T} = \mathrm{M_{TP}} + \mathrm{M_{TS}} = GJ\frac{d\beta_1}{dy_1} - EC_\omega \frac{d^3\beta_1}{dy_1^3}, \tag{2.2a}$$

where $\mathrm{M_T}$ is total twisting moment, $\mathrm{M_{TP}}$ is primary twisting moment due to uniform torsion, $\mathrm{M_{TS}}$ is secontary twisting moment due to warping restraint.

For an element with constant $\mathrm{M_T}$, the warping torsion $\mathrm{M_{TS}}$ generates a generalized force called Bimoment $\left(\mathrm{M_\omega}\right)$ as follows:

$$\mathrm{M_\omega} = -EC_\omega \frac{d^2\beta_1}{dy_1^2}. \tag{2.3b}$$

The total shear stress $\sigma_{12\mathrm{T}}$ due to torsion is the sum of the primary shear stress $\sigma_{12\mathrm{p}}$ due to the primary twisting moment for open section and the secondary shear stress $\sigma_{12\mathrm{s}}$ due to the secondary twisting moment for warping restraints.

$$\sigma_{12\mathrm{T}} = \sigma_{12\mathrm{p}} + \sigma_{12\mathrm{s}}. \tag{2.3}$$

Consider the homogeneous form of the governing equation (2) and let the characteristic number for torsion of a bar be defined as follows:

$$EC_\omega \frac{d^4\beta_1}{dy_1^4} - GJ\frac{d^2\beta_1}{dy_1^2} = 0,$$
$$\frac{d^4\beta_1}{dy_1^4} - \left(\frac{\theta}{a}\right)^2 \frac{d^2\beta_1}{dy_1^2} = 0, \tag{2.4}$$
$$\theta := a\sqrt{\frac{GJ}{EC_\omega}},$$

where θ is characteristic number for torsion, a is length of the bar.

The general solution for the homogeneous equation (2.4) is satisfied by the following assumed twisting angle function $\beta_1\left(\mathrm{y_1}\right)$ and it yields to the exact solutions of the angle of twists, its derivatives, twisting moments, and bimoments of a node. They are given by

$$\beta_1 = c_1 \sinh\frac{\theta y_1}{a} + c_2 \cosh\frac{\theta y_1}{a} + c_3\frac{y_1}{a} + c_4. \quad (2.5)$$

Based on the derivatives of equation (2.5) the following equations are obtained:

$$\frac{d\beta_1}{dy_1} = c_1\left(\frac{\theta}{a}\right)\cosh\frac{\theta y_1}{a} + c_2\left(\frac{\theta}{a}\right)\sinh\frac{\theta y_1}{a} + c_3\frac{1}{a}, \quad (2.6)$$

$$\frac{d^2\beta_1}{dy_1^2} = c_1\left(\frac{\theta}{a}\right)^2\sinh\frac{\theta y_1}{a} + c_2\left(\frac{\theta}{a}\right)^2\cosh\frac{\theta y_1}{a}, \quad (2.7)$$

$$\frac{d^3\beta_1}{dy_1^3} = c_1\left(\frac{\theta}{a}\right)^3\cosh\frac{\theta y_1}{a} + c_2\left(\frac{\theta}{a}\right)^3\sinh\frac{\theta y_1}{a}, \quad (2.8)$$

$$\frac{d^4\beta_1}{dy_1^4} = c_1\left(\frac{\theta}{a}\right)^4\sinh\frac{\theta y_1}{a} + c_2\left(\frac{\theta}{a}\right)^4\cosh\frac{\theta y_1}{a}. \quad (2.9)$$

The free coefficients c_1 to c_4 are determined so that the boundary conditions at the ends of the bar are satisfied. If the vertex $y_1 = 0$ is fixed and a twisting moment M_T is applied at vertex $y_1 = a$ which is free to warp. Solving equation (2.5) with the boundary conditions and the free coefficients are given below:

$$c_3 = \frac{M_T a}{GJ},\ c_1 = -\frac{c_3}{\theta},\ c_2 = \frac{c_3}{\theta}\tanh\theta,\ c_4 = -\frac{c_3}{\theta}\tanh\theta.$$

These coefficients are substituted into expression (2.5) and the angle of twist is given below:

$$\beta_1 = \frac{M_T a}{GJ\theta}\left(\tanh\theta\left(\cosh\frac{\theta y_1}{a} - 1\right) - \left(\sinh\frac{\theta y_1}{a} - \frac{y_1}{a}\right)\right). \quad (2.10)$$

Based on equation (2.10), the following equations of M_{TP}, M_{Ts} and M_ω for a node are obtained.

$$M_{TP} = M_T + M_T\left(\tanh\theta\sinh\frac{\theta y_1}{a} - \cosh\frac{\theta y_1}{a}\right), \quad (2.11)$$

$$M_{TS} = -M_T\left(\tanh\theta\sinh\frac{\theta y_1}{a} - \cosh\frac{\theta y_1}{a}\right), \quad (2.12)$$

$$M_\omega = -\frac{M_T\theta}{a}\left(\tanh\theta\cosh\frac{\theta y_1}{a} - \sinh\frac{\theta y_1}{a}\right). \quad (2.13)$$

2.2. Numerical case studies

In this study, the variation of M_{TP}, M_{TS} and M_ω with different value of θ is investigated. Different section types are considered as it is given in Table 5 and the section properties, displacements, rotations, stresses are to be compared for all cases in addition their distribution with in the span is compared based on their values of θ. Tables 1 to 3 show comparatively for different value of θ along the span of the beam, the initial value of θ is 1 and the maximum is 10. The variation of M_{TP}, M_{TS} and M_ω for different value of θ are presented. The results are tabulated below to bars of closed and/or open sections of thin walled steel cross section subjected to different torsional loading and to the most general torsional boundary conditions. In Table 1, the values are obtained based on equation (2.11) as it is expressed in a dimensionless form for diverse values of θ as shown below.

Table 1. Variation of M_{TP} for different value of θ.

y_1/a	M_{TP} / M_T				
	θ = 1	θ = 2.5	θ = 5	θ = 7.5	θ = 10
0	1.00	1.00	1.00	1.00	1.00
0.2	0.87	0.61	0.37	0.22	0.14
0.4	0.77	0.38	0.14	0.05	0.02
0.6	0.70	0.25	0.05	0.01	0.00
0.8	0.66	0.18	0.02	0.00	0.00
1	0.65	0.16	0.01	0.00	0.00

Similarly, In Table 2 and Tables 3–4, the values are obtained based on equations (2.12) and (2.13) respectively and they are expressed in a dimensionless form for different values of θ as shown below.

Table 2. Variation of M_{TS} for different value of θ.

y_1/a	M_{TS} / M_T				
	θ = 1	θ = 2.5	θ = 5	θ = 7.5	θ = 10
0	0.00	0.00	0.00	0.00	0.00
0.2	0.13	0.39	0.63	0.78	0.86
0.4	0.23	0.62	0.86	0.95	0.98
0.6	0.30	0.75	0.95	0.99	1.00
0.8	0.34	0.82	0.98	1.00	1.00
1	0.35	0.84	0.99	1.00	1.00

Table 3. Variation of M_ω for different value of θ with θ/α = 2.

y_1/a	M_ω / M_T				
	θ = 1	θ = 2.5	θ = 5	θ = 7.5	θ = 10
0	–0.38	–0.49	–0.50	–0.50	–0.50
0.2	–0.29	–0.30	–0.18	–0.11	–0.07
0.4	–0.21	–0.17	–0.07	–0.02	–0.01
0.6	–0.13	–0.10	–0.02	–0.01	0.00
0.8	–0.07	–0.04	–0.01	0.00	0.00
1	0.00	0.00	0.00	0.00	0.00

Table 4. Variation of M_ω for different value of θ with θ/α = 4.

y_1/a	M_ω / M_T				
	θ = 1	θ = 2.5	θ = 5	θ = 7.5	θ = 10
0	–0.19	–0.25	–0.25	–0.25	–0.25
0.2	–0.14	–0.15	–0.09	–0.06	–0.03
0.4	–0.10	–0.09	–0.03	–0.01	0.00
0.6	–0.07	–0.05	–0.01	0.00	0.00
0.8	–0.03	–0.02	0.00	0.00	0.00
1	0.00	0.00	0.00	0.00	0.00

According to equation (2.5), with the solution function for $\beta_1(y_1)$ and replacing the integration constants with the deformations, the following stuffiness relation is obtained. Considering the non-uniform torsion, the warping effect is contained within through an additional degree of freedom at each nodal point of the beam.

$$K_T = \frac{EC_\omega}{a^3} \begin{vmatrix} k_{T1} & k_{T2} & k_{T3} & k_{T4} \\ k_{T2} & k_{T6} & k_{T7} & k_{T8} \\ k_{T3} & k_{T7} & k_{T11} & k_{T12} \\ k_{T4} & k_{T8} & k_{T12} & k_{T16} \end{vmatrix}$$

$$K_{T1} = K_{T11} = S*\theta\sinh\theta,\ K_{T6} = K_{T16} = S*(\cosh\theta - \frac{\sinh\theta}{\theta})*a^2$$

$$K_{T2} = K_{T4} = S*(\cosh\theta - 1)*a,\ K_{T8} = S*\left(\frac{\sinh\theta}{\theta} - 1\right)*a^2$$

$$S = \left(\frac{\theta^2}{Q}\right),\ Q = 2(1-\cosh\theta) + \theta\sinh\theta,\ K_{T3} = -K_{T1},\ K_{T7} = K_{T12} = -K_{T2}$$

Different section types are given in Table 5 which are the I section, rectangular hollow section, and channel section. Considering the prismatic bar of Fig. 1 as it is fixed at vertex $y_1 = 0$ and subjected to a twisting moment of M_T without warping restraint at vertex $y_1 = a$. The section properties, displacements, rotations, stresses are to be compared for all cases and compared their distribution within the span based on the required value of θ.

Table 5. Different section types.

Section type	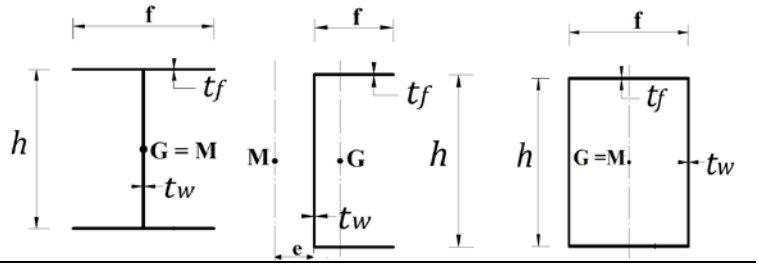		
h(mm)	400	400	400
f(mm)	180	180	180
t_f(mm)	11	11	11
t_w(mm)	8	8	8
$E = 200*10^6\ kN/m^2$	$M_T = 1.0\ kN\,m$	$G = 77*10^6\ kN/m^2$	

3. Results and Discussions

3.1. The variation of M_{TP}, M_{TS} and M_ω for different value of θ

The behavior and variation of M_{TP} and M_{Ts} for different value of θ which ranges from 1 to 10 are presented graphically in Fig. 2. Considering a point nearly to the support at $y_1 = 0$ for Fig. 1, the total torsional moment is largely carried by the primary twisting moment, whereas the secondary twisting moment is small. At points in the span, the torsion is carried partly as St. Venant torsion (i.e. by the St. Venant shear stresses) and partly as warping torsion (i.e. by the shear stresses caused by the restraint of warping. For θ=L both torsion mechanisms contribute to M_T throughout the beam in both cases but with the increasing of the value of θ the influence of the twisting moment role to the M_T varies as shown in the Fig. 2. In view of Fig. 2 (a) with increasing of θ value of M_{TP} reduces fast and the torsional moment is dominated by St. Venant in a major part of the beam. Similarly, in Fig. 2(b), with the increasing value of θ, the St. Venant moment is growing, and the torsional moment M_T is dominated by St. Venant in a major part of the beam in both cases.

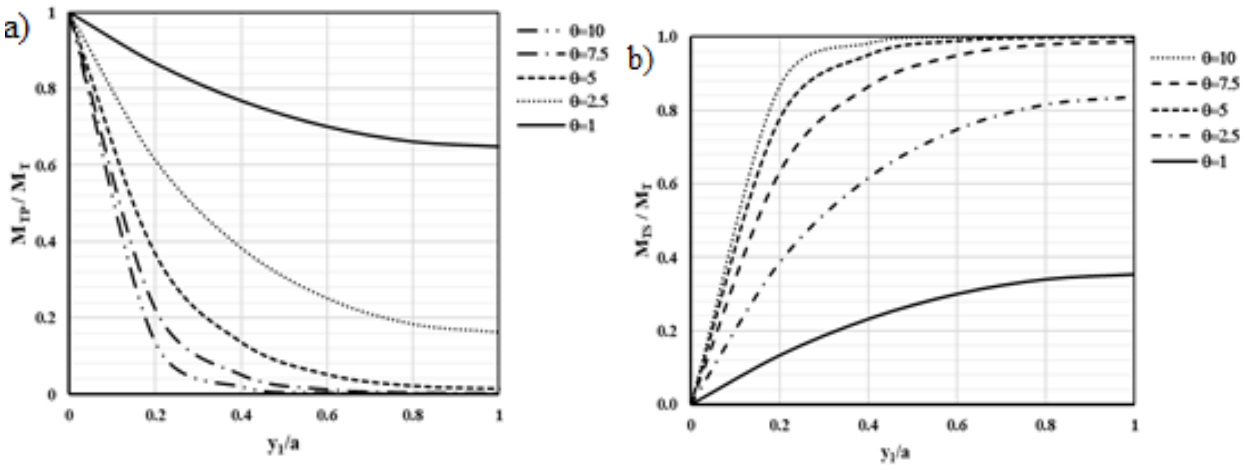

Figure 2. Variation of M_{TP} and M_{TS} for different value of θ.

Similarly, the behavior and variation of warping moment (M_ω) for different value of θ which ranges from 1 to 10 are presented graphically in Fig. 3 As the characteristics number for torsion (θ) is an indicator of how quickly the effect of warping restraint dissipates because the warping moment varies based on the restrained conditions of the beam. The variation of M_ω in the Fig. 3 displays the greater values at the fixed support where the warping is prevented and induces the largest normal stresses. At the free end the beam can warp freely as a result the normal stresses is zero, thus $M_\omega(a)=0$. The two graphs below are plotted for different value of θ/a (i.e. θ/a = 2 and 4) as it is for general case. The distribution of M_ω varies differently in both cases with varying values of θ and thus the normal warping stress differs along the beam based on the position of restrained torsion and section type.

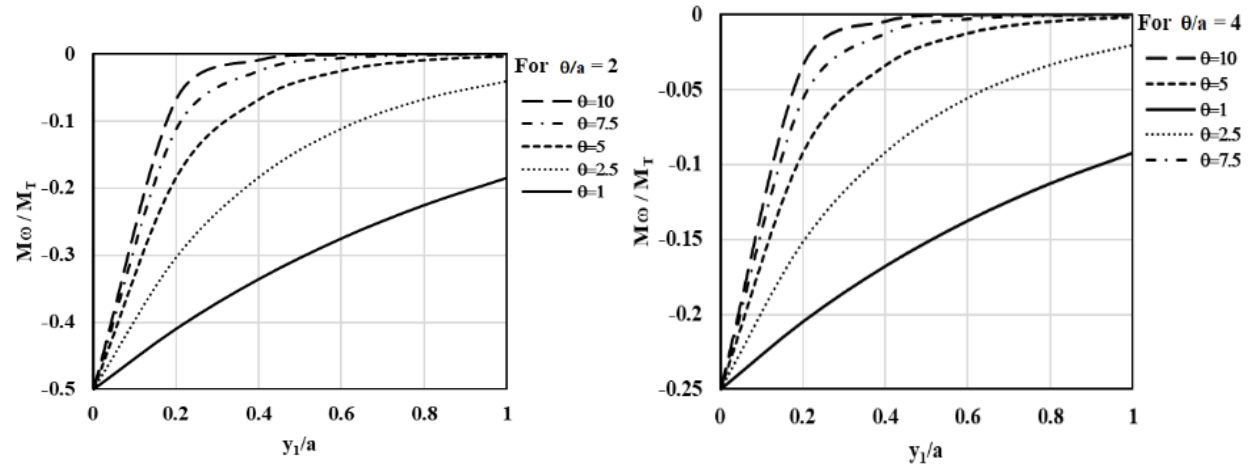

Figure 3. Variation of M_ω for different value of θ.

3.2. Comparison of M_T components with three different thin walled sections

The section properties, displacements, rotations, stresses are to be compared for all cases and compared their distribution with the span based on the required value of θ.

Case I: Refereeing Table 5, for an I- sections, the values of C_ω, J, θ and $\beta_1(a)$ are computed below:

$$C_\omega=\frac{1}{24}t_f b^3 h^2=0.4277*10^{-6}\,\mathrm{m}^6,\ J=\frac{1}{3}(2ft_f{}^3+ht_w{}^3)=0.2280*10^{-6}\,\mathrm{m}^4,$$

$$\theta_{\mathrm{Isec.}}=1.812,$$

$$\beta_1=-0.1257\sinh 1.812+0.119208\cosh 1.812+0.2278-0.119208,$$

$$\beta_1=0.109\ \text{radians}=6.25\ \text{degrees}.$$

The angle of twist for uniform torsion of an I-section of the bar is:

$$\beta_{1,\text{uniform}} = \frac{a\,M_T}{G\,J} = \frac{4.0}{77*10^6 \bullet .228*10^{-6}} = 0.228 \text{ radians} = 13.06 \text{ degrees}$$

The variation of the uniform, non-uniform angle of twist, M_{TP}, M_{Ts} and M_T on the axis of the bar are shown in Fig. 4. The rotation at vertex $y_1 = a$ due to non-uniform torsion is around 50 percent of the rotation for uniform torsion of an I-section. Both M_{TP} and M_{Ts} contribute to M_T through the span of the beam and the torsional stresses are due to St Venant shear stresses and the restraint of warping. The applied twisting moment is resisted entirely by the secondary twisting moment at support $(y_1 = 0)$ and entirely by the primary twisting moment at $y_1 = a$. According to the studies on [18, 27], our results for the variation of the uniform, non-uniform angle of twist, M_{TP}, M_{Ts} and M_ω on the axis are compared for further verifications and the results are some. The distribution of the total moment between uniform and non-uniform torsion at intermediate points is shown in Fig. 4.

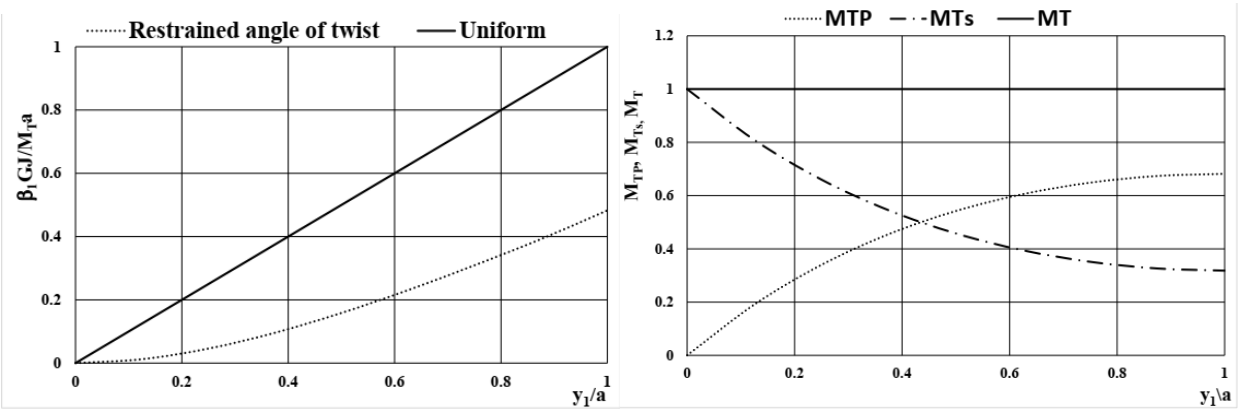

Figure 4. The normalised graphs of β_1, M_{TP}, M_{TS} and M_T of restrained I-beam section.

Furthermore, the values of β_1 of equation 2.5 and its derivatives are plotted in Fig. 5 to show their comparisons and behaviours along the length of the member. The behaviour of the flanges can be observed in the graph for β_1 and its first derivatives (β_1'). They show the variation in twist to which St. Venant shear strains and stresses are proportional to the primary torsional moments. The curvature of the flanges is also associated with the graph β_1'' and it is proportional to the warping moment in one flange. A combined graph for β_1' and β_1''' is shown in the Fig. 5(b) so β_1' is representing for the primary twisting moment and β_1''' belongs to the secondary twisting moments. The graph of β_1''' belongs to the characteristics of the rate of change of curvature and it is proportional to the warping shear force in the flange in addition to the warping torsional moment. Based on the Fig. 5(b) β_1' contributes 68 % and β_1''' contributes 32 % of the total torsional moment.

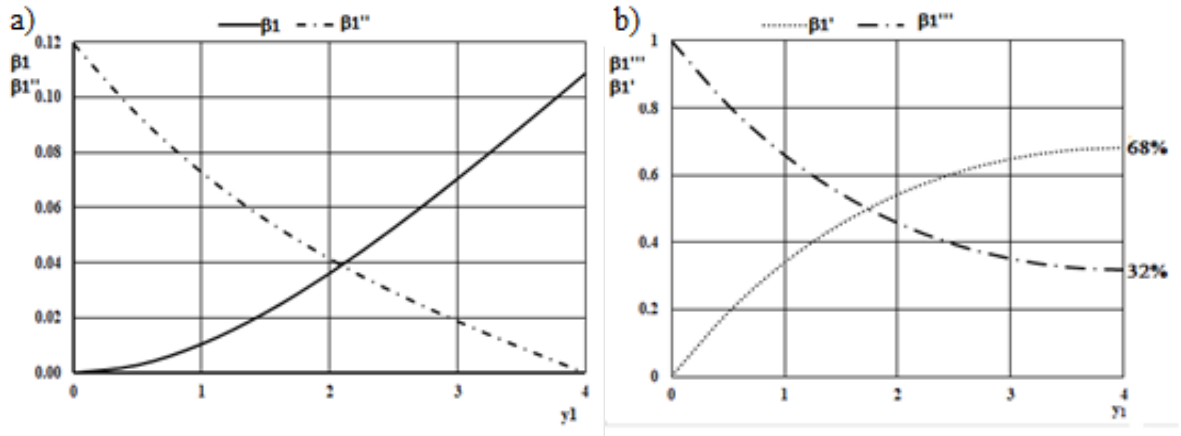

Figure 5. Decomposition of total twisting moment for an I-beam.

For an I-section, the longitudinal stress σ_{11} at $y_1 = 0$ due to non-uniform torsion and the warping function are computed as below:

$$\omega = \pm\frac{1}{4} f\, h = \pm 18.0 * 10^{-3}\ \mathrm{m}^2,$$

$$\sigma_{11} = -\omega\frac{M_T}{C_\omega}\tanh\theta\left(\frac{a}{\theta}\right) = \pm 0.0980 * 10^{6}\ \mathrm{kN/m^2}$$

The primary shear stress at the free end $(y_1 = a)$ is computed as given below and it varies linearly over the thickness of the walls of the section.

$$\text{flange:} \quad \tau_{max} = \pm\frac{M_T\, t_f}{J} = \pm 48.2\ \mathrm{N/mm^2},$$

$$\text{web:} \quad \tau_{max} = \pm\frac{M_T\, t_w}{J} = \pm 35.1\ \mathrm{N/mm^2}$$

The secondary shear stress at node $y_1 = 0$ is computed by determining the static moments of the warping function and it is constant over the thickness of the walls of the section. The contributions of the walls to the static moment of the warping function are computed based on the shear flow at the external vertices. The shear stress due to warping restraint is:

$$\sigma_{12s} = \frac{F_\omega}{t_f} = -\frac{20.83}{0.011} = -1893.6\ \mathrm{kN/m^2} = -1.9\ \mathrm{N/mm^2}$$

The distributions of the stress σ_{11}, warping function (ω) and secondary shear stresses σ_{11} over the section due to the non-uniform torsion are shown in Fig. 6.

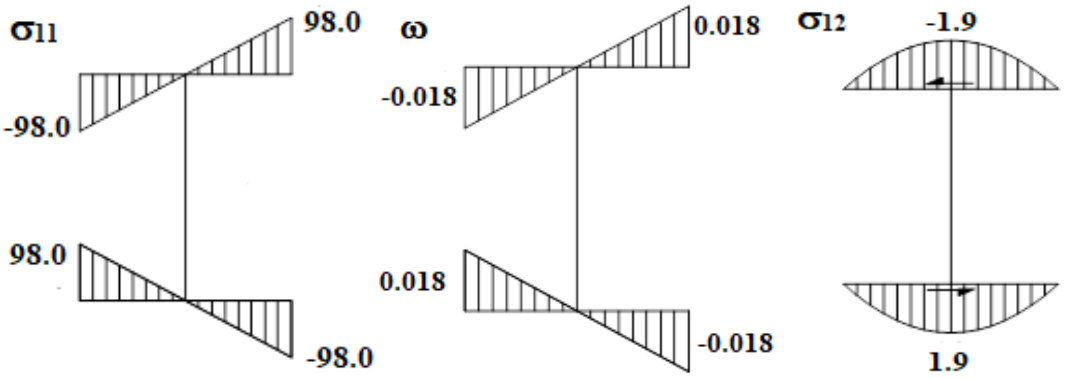

Figure 6. Distribution of σ11, ω and σ12p $(\mathrm{N/mm^2})$.

Case II: Similarly, for rectangular hollow cross-section, which is given in Table 5, the values for C_ω, J, θ and $\beta_1(a)$ are computed below:

$$C_\omega = \frac{2}{3}\omega_0^2(f\, t_f + h\, t_w) = 0.2875 * 10^{12}\ \mathrm{mm^6},$$

$$J = \frac{2 f^2 h^2 t_w t_f}{f\, t_w + h\, t_f} = 0.1562 * 10^{9}\ \mathrm{mm^4}$$

$$\theta_{Rec.sec.} = 57.85$$

$$\beta_1 = 5.749 * 10^{-6} \bullet (-\sinh 57.85 + \cosh 57.85 - 1.0) + 0.3326 * 10^{-3}$$

$$\beta_1 = 0.327 * 10^{-3}\ \text{radians} = 0.0187\ \text{degrees}$$

The angle of twist for uniform torsion of the rectangular section of the bar is:

$$\beta_{1,uniform} = \frac{a\, M_T}{G\, J} = \frac{4.0}{77 * 10^{6} \bullet 0.1562 * 10^{-3}} = 0.333 * 10^{-3}\ \text{radians}$$

The variation of the uniform and non-uniform angle of twist (restrained torsion) on the axis of rectangular hollow cross-section of the bar are shown in Fig. 7. For rectangular hollow cross-section as the value of θ is large and the angle of twist is very small in its magnitude. The angle of twist at points nearer to the support has significant magnitude as shown in the Fig. 7 and suddenly drops to a small value at the free end. The rotation at vertex $y_1 = a$ due to uniform and non-uniform torsion is almost the same and its magnitude is negligible comparing with an open section.

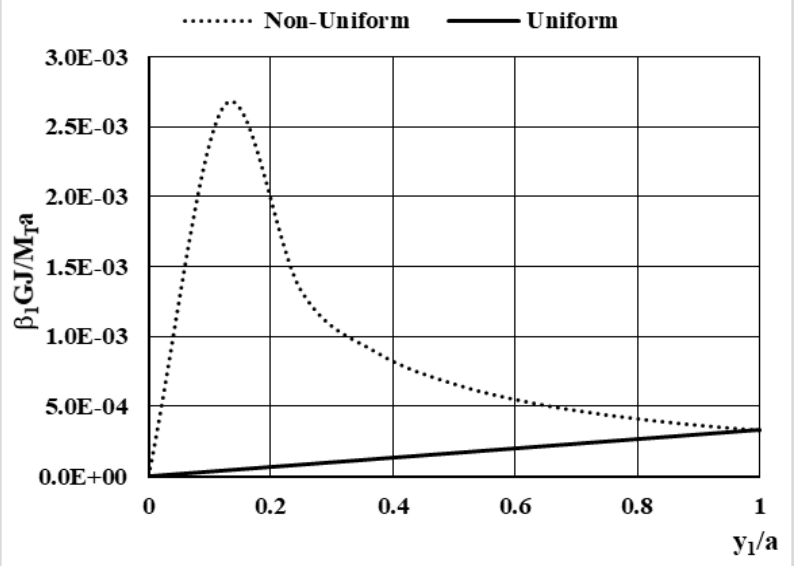

Figure 7. The normalised graphs of β_1 of restrained rectangular hollow cross-section.

The longitudinal stress σ_{11} at $y_1 = 0$ due to non-uniform torsion of rectangular hollow section is given below and the distribution of this stress over the section is shown in Fig. 8:

$$\omega_0 = \frac{1}{4} f\, h \frac{\mu - 1}{\mu + 1}$$

$$\text{with} \quad \mu := \frac{h}{t_w}\frac{t_f}{f} \quad \omega = \pm\omega_0 = \pm 9.124 * 10^{-3}\ \text{m}^2$$

$$\sigma_{11} = -\omega \frac{M_T}{C_\omega} \tanh\theta\left(\frac{a}{\theta}\right) = \mp 2.2\ \text{N/mm}^2$$

The primary shear stress is null at $y_1 = a$ and it is computed with expressions shown below. It is constant over the thickness of the walls of the section.

$$\text{flange}: \sigma_{12p} = \frac{M_T}{2 f\, h\, t_f} = \pm 0.63\ \text{N/mm}^2,$$

$$\text{web}: \sigma_{12p} = \frac{M_T}{2 f\, h\, t_w} = \pm 0.86\ \text{N/mm}^2$$

The secondary shear stresses (σ_{12}) at the support $(y_1 = 0)$ depend on the Static moments (S_ω) of the warping function. The increments of the static moment for the walls are given by the expression below:

$$\eta = \frac{180}{11} + \frac{400}{8} = 66.36$$

$$S_0 = -\frac{9.124*10^{-3}}{6 \bullet 66.36} \bullet (0.18^2 - 0.40^2) = -2.92*10^{-6}\ m^4$$

$$\text{wall AB}: S_{(1)} = S_0 - \frac{1}{4}\omega_0\, f\, t_f = -2.92*10^{-6} - 4.516*10^{-6} = -7.44*10^{-6} m^4$$

$$\text{wall BC}: S_{(2)} = S_0 + \frac{1}{4}\omega_0\, f\, t_w = -2.92*10^{-6} + 7.299*10^{-6} = 4.38*10^{-6} m^4$$

Based on the above solutions and static moment of the section, the variations of secondary shear stress over the section are shown in Fig. 8:

$$\sigma_{12s} = -\frac{M_T}{t}\frac{S_\omega}{C_\omega} = -\frac{1.0}{0.2875*10^{-6}}\frac{S_\omega}{t} = -3.4783*10^6 \frac{S_\omega}{t}\ kN/m^2$$

The distributions of the stress σ_{11}, warping function (ω) and secondary shear stresses σ_{12} over the section due to the non-uniform torsion are shown in Fig. 8.

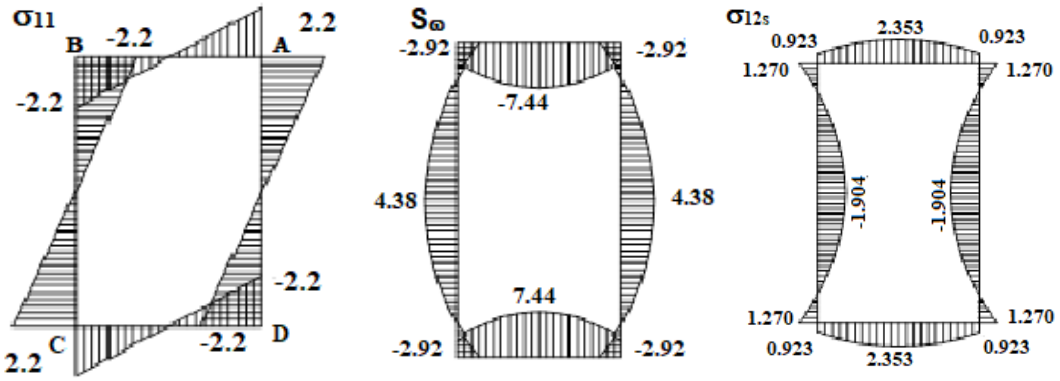

Figure 8. Stress (σ_{11}) (a), Static moments (S_ω), secondary shear stress (σ_{12s}) (N/mm^2).

Case III: Likewise, by considering the channel section of Table 5, the values for C_ω, J, θ and $\beta_1(a)$ are calculated as given below:

$$C_\omega = \frac{\left(f - \frac{t_w}{2}\right)^3 * h^2 * t_f}{12}\left[\frac{2ht_w + 3\left(f - \frac{t_w}{2}\right)t_f}{ht_w + 6\left(f - \frac{t_w}{2}\right)t_f}\right] = 0.580*10^{-6}\ m^6,$$

$$J = \frac{1}{3}(2f\, t_f^{\,3} + h\, t_w^{\,3}) = 0.218*10^{-6}\ m^4$$

$$\theta = 1.52$$

$$\beta_1 = -0.157 \sinh 1.52 + 0.142 \cosh 1.52 + 0.238 - 0.142$$

$$\beta_1 = 0.083 \text{radians} = 4.75 \text{ degrees}$$

The angle of twist for uniform torsion of the rectangular section bar is:

$$\beta_{1,\text{uniform}} = \frac{a M_T}{G J} = \frac{4.0}{77*10^6 \times 0.218*10^{-3}} = 0.24 \text{ radians} = 13.75 \text{ degrees}$$

The variation of the uniform and non-uniform angle of twist (restrained torsion) on the axis of the channel section of a bar is shown in Fig. 9. The rotation at vertex $y_1 = a$ due to non-uniform torsion is 40 percent of the rotation for uniform torsion of the channel section.

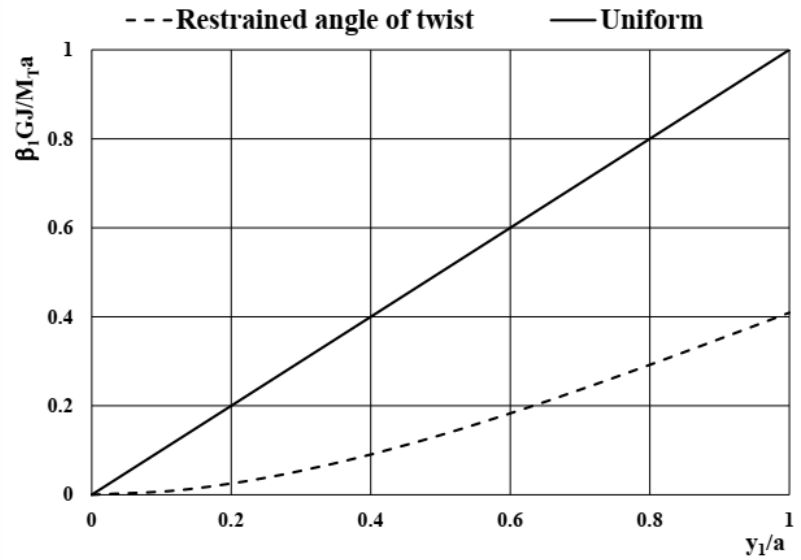

Figure 9. The normalised graphs of β_1 of restrained Chunnel section.

For channel section, the longitudinal stress (σ_{11}) at $y_1 = 0$ due to non-uniform torsion and the warping function are computed as below:

$$\omega_A = \frac{h}{2} * (f - t_w - e) = 21.4 * 10^{-3} m^2$$

$$\omega_B = -e * \frac{h - t_f}{2} = -13.8 * 10^{-3} m^2$$

$$\sigma_{11A} = \omega_A \frac{M_T}{C_\omega} \tanh\theta \left(\frac{a}{\theta}\right) = 124.6 \ N/mm^2$$

$$\sigma_{11B} = -\omega_B \frac{M_T}{C_\omega} \tanh\theta \left(\frac{a}{\theta}\right) = -80.3 \ N/mm^2$$

The values and distribution of the warping function at the external vertices and longitudinal stress are given in Fig. 8: Correspondingly the primary shear stress in the flange and web plates at support is zero and at node $y_1 = a$ is computed as follow. It varies linearly over the thickness of the walls of the section.

$$\text{flange}: \quad \tau_{max} = \pm \frac{M_T \, t_f}{J} = \pm \frac{0.011}{0.218 * 10^{-6}} \ kN/m^2 \ \hat{=} \ \pm 50.0 \ N/mm^2$$

$$\text{web}: \quad \tau_{max} = \pm \frac{M_T \, t_w}{J} = \pm \frac{0.008}{0.218 * 10^{-6}} \ kN/m^2 \ \hat{=} \ \pm 36.4 \ N/mm^2$$

The secondary shear stress is null at section and at node $y_1 = 0$ is computed by determining the static moments of the warping function.

$$S_0 = 0.5 t_f (f - 0.5 t_w) h * (0.5f - 0.25 t_w - e) = 7.36 * 10^{-6} \ m^4$$

$$\text{wall AB}: S_{(2)} = \frac{1}{4} h \, t_f \, [(f - 0.5 t_w) - e]^2 = 12.6 * 10^{-6} m^4$$

$$\text{wall BC}: S_{(1)} = S_0 - \frac{1}{8} t_w \, eh^2 = -3.68 * 10^{-6} m^4$$

$$\sigma_{12s0} = -\frac{M_T}{t_f}\frac{S_\omega}{C_\omega} = -1.01 N/m^2$$

$$\sigma_{12s1} = -\frac{M_T}{t_w}\frac{S_\omega}{C_\omega} = 0.07 N/m^2$$

$$\sigma_{12s2} = -\frac{M_T}{t_f}\frac{S_\omega}{C_\omega} = -1.15 N/m^2$$

The distributions of the stress σ_{11}, Static moments (S_ω) and secondary shear stresses σ_{11} over the section due to the non-uniform torsion are shown in Fig. 10.

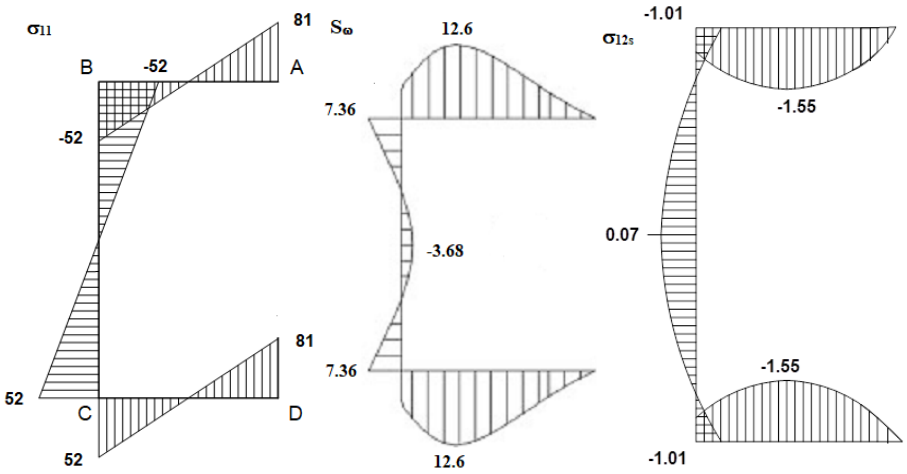

Figure 10. Stress (σ_{11}) , Static moments (S_ω), secondary shear stress (σ_{12s}) (N\mm^2).

A combined graph for angle of twist for closed and open sections is shown in Fig. 11 for both uniform and restrained torsion. The rotation at vertex $y_1 = a$ due to non-uniform torsion are 50 percent of the rotation for uniform torsion of I section and 40 percent of the rotation for uniform torsion of Chunnel section. For closed channels like rectangular hollow cross-section, the rotations in uniform and non-uniform torsions are considered negligible as their magnitudes are very small compared to the open cross sections as shown in Fig. 11.

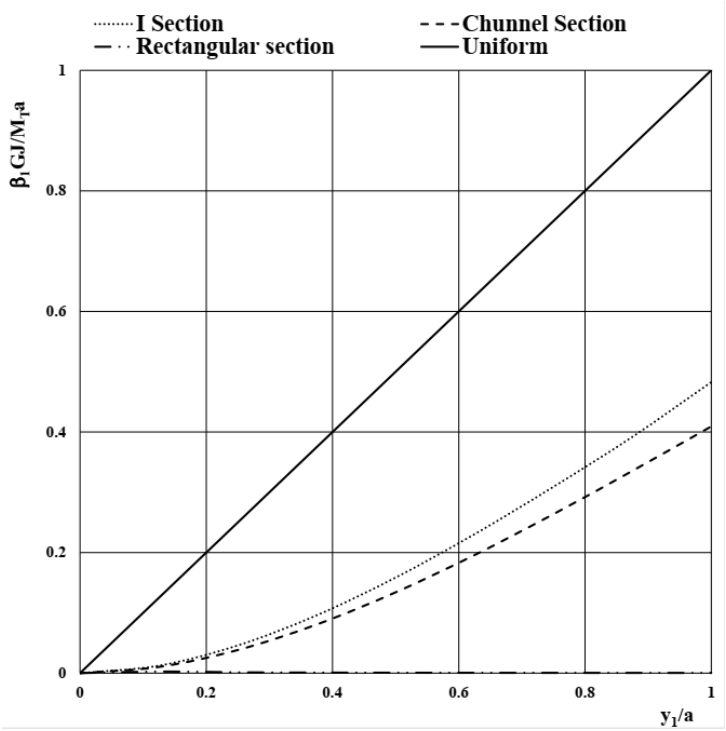

Figure 11. The combined normalised graphs of β_1 for all restrained section types.

In this study, the characteristic number for torsion is the main criteria to study the behaviour of a bar with restrained torsion and the variation of the uniform, non-uniform angle of twist, M_{TP}, M_{Ts} and M_{ω} on the axis of the bar are expressed as a function of the characteristic number for torsion and all results are compared with different studies [14, 15, 27]. From Fig. 11, the normalization graph clearly presents the combined graph for angle of twist for closed and open sections for both uniform and restrained torsion. For closed channels like rectangular hollow cross-section, the rotations are very small and are considered negligible but comparing to different studies [29, 43] it shows that the effect of warping must be considered in the case of non-uniform torsion of closed-section beams.

4. Conclusion

In this study, the characteristic number for torsion was adopted to study the behaviour of a bar with restrained torsion. The resulting responses from all cases using different value for the characteristic number for torsion were analyzed and compared. According to the previous findings, it is concluded that:

1. When considering fixed support conditions Vlasov torsion must be accounted as the behaviour for St. Venant and Vlasov torsion existing for all section types.

2. In this study, we used the hyperbolic than polynomial shape functions as it gave the exact results as the analytical solution.

3. With the increasing of θ value, M_{TP} reduces fast and the torsional moment is dominated by St. Venant in a major part of the beam but for θ = 1 both torsion mechanisms contribute to M_T. The distribution of $M\omega$ varies with the different values of θ and $\theta^* a$ consequently the normal warping stress differs along the beam based on the position of restrained torsion and section type.

4. The angle of twist of non-uniform torsion differs from uniform torsion by 50, 1.8, and 41 percents for the I-section, rectangular tube, and channel section, respectively.

5. Normal stresses dominate the stress within the bar as the cross-section is restrained and Vlasov shear stresses are very small and vanished when the normal stress reached maximum. Contradictory to this, at the free end the shear stress is dominated by St. Venant shear stresses and its maximum value is located at the mid of the flange.

6. The primary shear stress is considerably lower for the closed than open sections. The secondary shear stress is depending on the static moments of the warping function.

7. For closed channels like rectangular hollow cross-section, the rotation and warping are very small and are considered negligible but comparing to different studies it shows that the effect of warping must be considered in the case of non-uniform torsion of closed-section beams.

References

1. Pavlenko, A.D., Rybakov, V.A., Pikht, A.V., Mikhailov, E.S. Non-uniform torsion of thin-walled open-section multi-span beams. Magazine of Civil Engineering. 2016. 67 (7). Pp. 55–69. DOI: 10.5862/MCE.67.6
2. Vlasov, V.Z. Thin-walled Elastic Beams. Springfield, Va.: National Technical Information Service. Virginia,1984. 493 p.
3. Petrolo, A.S., Casciaro, R. 3D beam element based on Saint Venànt's rod theory. Computers and Structures. 2004. 82 (29–30). Pp. 2471–2481. DOI: 10.1016/j.compstruc.2004.07.004
4. Gebre, T.H., Galishnikova, V.V. The impact of section properties on thin-walled beam sections with restrained torsion. Journal of Physics: Conference Series. 2020. 1687 (1). DOI: 10.1088/1742-6596/1687/1/012020
5. Selyantsev, I.M., Tusnin, A. Cold-formed steel joints with partial warping restraint. Magazine of Civil Engineering. 2021. 101(1). 10101. DOI: 10.34910/MCE.101.1
6. El Fatmi, R. Non-uniform warping including the effects of torsion and shear forces. Part I: A general beam theory. International Journal of Solids and Structures. 2007. 44 (18–19). Pp. 5912–5929. DOI: 10.1016/j.ijsolstr.2007.02.006
7. Tsipiras, V.J., Sapountzakis, E.J. Bars under nonuniform torsion – Application to steel bars, assessment of EC3 guidelines. Engineering Structures. 2014. 60. Pp. 133–147. DOI: 10.1016/j.engstruct.2013.12.027.
8. Saadé, K., Espion, B., Warzée, G. Non-uniform torsional behaviour and stability of thin-walled elastic beams with arbitrary cross-sections. Thin-Walled Structures. 2004. 42 (6). Pp. 857–881. DOI: 10.1016/j.tws.2003.12.003
9. Tsipiras, V.J., Sapountzakis, E.J. Secondary torsional moment deformation effect in inelastic nonuniform torsion of bars of doubly symmetric cross-section by BEM. International Journal of Non-Linear Mechanics. 2012. 47 (4). Pp. 68–84. DOI: 10.1016/j.ijnonlinmec.2012.03.007. URL: http://dx.doi.org/10.1016/j.ijnonlinmec.2012.03.007
10. Lopez, F.L. A 3D Finite Beam Element for the Modelling of Composite Wind Turbine Wings. 2013.126 p.
11. Qi, H., Wang, Z., Zhang, Z. An Efficient Finite Element for Restrained Torsion of Thin-Walled Beams Including the Effect of Warping and Shear Deformation. IOP Conference Series: Earth and Environmental Science. 2019. 233 (3). DOI: 10.1088/1755-1315/233/3/032029
12. Murín, J., Aminbaghai, M., Kutiš, V., Královič, V., Sedlár, T., Goga, V., Mang, H. A new 3D Timoshenko finite beam element including non-uniform torsion of open and closed cross-sections. Engineering Structures. 2014. 59. Pp. 153–160. DOI: 10.1016/j.engstruct.2013.10.036

13. Sapountzakis, E.J. Bars under Torsional Loading: A Generalized Beam Theory Approach. ISRN Civil Engineering. 2013. 2013. Pp. 1–39. DOI: 10.1155/2013/916581
14. Pavazza, R., Matoković, A., Vukasović, M. A theory of torsion of thin-walled beams of arbitrary open sections with the influence of shear. Mechanics Based Design of Structures and Machines. 2020. 0 (0). Pp. 1–36. DOI: 10.1080/15397734.2020.1714449.
15. Kuttke, P., Kurfürst, A., Scheiner, S., Hellmich, C. Sequential 1D/2D Finite Element analyses of tramway rails under bending and restrained torsion, based on the principle of virtual power. Mechanics of Advanced Materials and Structures. 2019. 6494. DOI: 10.1080/15376494.2019.1647317
16. Mohareb, M., Nowzartash, F. Exact finite element for nonuniform torsion of open sections. Journal of Structural Engineering. 2003. 129 (2). Pp. 215–223. DOI: 10.1061/(ASCE)0733-9445(2003)129:2(215)
17. Sapountzakis, E.J., Tsipiras, V.J., Gkesos, P.G. Warping transmission in 3-D beam element including secondary torsional moment deformation effect. ECCOMAS Special Interest Conference – SEECCM 2013: 3rd South-East European Conference on Computational Mechanics, Proceedings – An IACM Special Interest Conference. 2013. Pp. 470–480.
18. Liping Wang1 and Ben Young, M.A. Restrained Torsion of Thin-Walled Beams. ASCE Journal of Structural Engineering. 2007. 1. Pp. 1–18. DOI: 10.1061/(ASCE)ST.1943-541X
19. Zojaji, A.R., Kabir, M.Z. Analytical approach for predicting full torsional behaviour of reinforced concrete beams strengthened with FRP materials. Scientia Iranica. 2012. 19 (1). Pp. 51–63. DOI: 10.1016/j.scient.2011.12.004.
20. Askandar, N.H., Mahmood, A.D., Kurda, R. Behaviour of RC beams strengthened with FRP strips under the combined action of torsion and bending. European Journal of Environmental and Civil Engineering. 2020. Pp. 1–17. DOI: 10.1080/19648189.2020.1847690.
21. Ganganagoudar, A., Mondal, T.G., Suriya Prakash, S. Analytical and finite element studies on behaviour of FRP strengthened RC beams under torsion. Composite Structures. 2016. 153. Pp. 876–885. DOI: 10.1016/j.compstruct.2016.07.014.
22. Alabdulhady, M.Y., Sneed, L.H., Carloni, C. Torsional behaviour of RC beams strengthened with PBO-FRCM composite – An experimental study. Engineering Structures. 2017. 136. Pp. 393–405. DOI: 10.1016/j.engstruct.2017.01.044.
23. Ubaydulloyev, M.N. Calculations of strengthened open profile thin-walled element enclosing structures. Magazine of Civil Engineering. 2014. 52 (8). DOI: 10.5862/MCE.52.6
24. Al-Rousan, R., Abo-Msamh, I. Impact of anchored CFRP on the torsional and bending behaviour of RC beams. Magazine of Civil Engineering. 2020. 96 (4). Pp. 79–93. DOI: 10.18720/MCE.96.7
25. Al-Rousan, R., Abo-Msamh, I. Bending and torsion behaviour of CFRP strengthened RC beams. Magazine of Civil Engineering. 2019. 92(8). Pp. 48–62. DOI: 10.18720/MCE.92.4
26. Banić, D., Turkalj, G., Brnić, J. Finite element stress analysis of elastic beams under non-uniform torsion. Transactions of Famena. 2016. 40 (2). Pp. 71–82. DOI: 10.21278/TOF.40206
27. Gunnlaugsson, G.A., Pedersen, P.T. A finite element formulation for beams with thin-walled cross-sections. Computers and Structures. 1982. 15 (6). Pp. 691–699. DOI: 10.1016/S0045-7949(82)80011-4.
28. Chen, S., Ye, Y., Guo, Q., Cheng, S., Diao, B. Nonlinear model to predict the torsional response of U-shaped thin-walled RC members. Structural Engineering and Mechanics. 2016. 60 (6). Pp. 1039–1061. DOI: 10.12989/sem.2016.60.6.1039
29. Murín, J., Kutiš, V., Královič, V., Sedlár, T. 3D beam finite element including nonuniform torsion. Procedia Engineering. 2012. 48. Pp. 436–444. DOI: 10.1016/j.proeng.2012.09.537
30. Aminbaghai, M., Murin, J., Kutiš, V., Hrabovsky, J., Kostolani, M., Mang, H.A. Torsional warping elastostatic analysis of FGM beams with longitudinally varying material properties. Engineering Structures. 2019. 200 (April). Pp. 109694. DOI: 10.1016/j.engstruct.2019.109694.
31. Murin, J., Aminbaghai, M., Hrabovsky, J., Mang, H. Second-order torsional warping modal analysis of thin-walled beams. COMPDYN 2017 – Proceedings of the 6th International Conference on Computational Methods in Structural Dynamics and Earthquake Engineering. 2017. 1. Pp. 1–19. DOI: 10.7712/120117.5406.16926
32. Emre Erkmen, R., Mohareb, M. Torsion analysis of thin-walled beams including shear deformation effects. Thin-Walled Structures. 2006. 44 (10). Pp. 1096–1108. DOI: 10.1016/j.tws.2006.10.012
33. El Fatmi, R. Non-uniform warping including the effects of torsion and shear forces. Part II: Analytical and numerical applications. International Journal of Solids and Structures. 2007. 44 (18–19). Pp. 5930–5952. DOI: 10.1016/j.ijsolstr.2007.02.005.
34. Pavazza, R., Matoković, A. Bending of thin-walled beams of the open section with the influence of shear, part I: Theory. Thin-Walled Structures. 2017. 116. Pp. 357–368. DOI: 10.1016/j.tws.2016.08.027
35. Ritchie, S.J.K., Leevers, P.S. Non-uniform and dynamic torsion of elastic beams. Part 1: Governing equations and particular solutions. Journal of Strain Analysis for Engineering Design. 1999. 34 (5). Pp. 303–311. DOI: 10.1243/0309324991513641
36. Wang, Z.Q., Zhao, J.C., Gong, J.H. A new torsion element of thin-walled beams including shear deformation. Applied Mechanics and Materials. 2011. 94–96. Pp. 1642–1645. DOI: 10.4028/www.scientific.net/AMM.94-96.1642
37. Wang, Z.Q., Zhao, J.C., Zhang, D.X., Gong, J.H. Restrained torsion of open thin-walled beams including shear deformation effects. Journal of Zhejiang University: Science A. 2012. 13 (4). Pp. 260–273. DOI: 10.1631/jzus.A1100149
38. Prokić, A., Mandić, R., Vojnić-Purčar, M., Folić, R. Torsional buckling of thin-walled beams in presence of bi-moment induced by axial loads. Computers & Smctures.1993. Vol. 47. No. 6. pp. 1065–1070.
39. Murin, J., Sedlar, T., Kralovic, V., Goga, V., Kalas, A., Aminbaghai, M. Numerical analysis and measurement of non-uniform torsion. Civil-Comp Proceedings. 2012. 99. Pp. 1–18. DOI: 10.4203/ccp.99.11
40. Floros, M.W., Smith, E.C. Finite element modelling of open-section composite beams with warping restraint effects. AIAA Journal. 1997. 35 (8). Pp. 1341–1347. DOI: 10.2514/2.242
41. Lalin, V.V., Rybakov, V.A., Ivanov, S.S., Azarov, A.A. Mixed finite-element method in V.I. Slivker's semi-shear thin-walled bar theory. Magazine of Civil Engineering. 2019. 89 (5). Pp. 79–93. DOI: 10.18720/MCE.89.7
42. Sapountzakis, E.J. Solution of non-uniform torsion of bars by an integral equation method. Computers and Structures. 2000. 77 (6). Pp. 659–667. DOI: 10.1016/S0045-7949(00)00020-1
43. Rubin, H. Torsions-Querschnittswerte für rechteckige Hohlprofile nach en 10210-2:2006 und en 10219-2:2006. Stahlbau. 2007. 76 (1). Pp. 21–33. DOI: 10.1002/stab.200710004

Contacts:

Vera Galishnikova, GalishnikovaVV@mgsu.ru

Tesfaldet Hadgembes Gebre, tesfaldethg@gmail.com

Received 27.09.2020. Approved after reviewing 08.04.2021. Accepted 04.06.2021.